Supporting Information

A Bi-metallic MOF Catalyst *via* Sensitive Detection & Adsorption of Fe^{3+} Ions for Size-selective Reaction Prompting

Yang Li,[a] *Ziling Chang,*[a] *Fangmin Huang,*[a] *Pengyan Wu,*[a,*] *Huacong Chu*[a] *and Jian Wang*[a,*]

[a]School of Chemistry and Materials Science & Jiangsu Key Laboratory of Green Synthetic Chemistry for Functional Materials, Jiangsu Normal University, Xuzhou, 221116, P. R. China.

E-mail: wpyan@jsnu.edu.cn (P.Y. Wu); wjian@jsnu.edu.cn (J. Wang)

Additional experimental details.

Reagents and chemicals: All reagents and solvents were of AR grade and used without further purification unless otherwise noted. 5,5'-methylenebisophthalic acid was synthesized according to the literature methods. (*Eur. J. Org. Chem.*, **2007**, *20*, 3271-3276) $Cd(ClO_4)_2{\cdot}6H_2O$ was purchased from Alfa Aesar, $Fe(NO_3)_3{\cdot}9H_2O$ and the other metal salts were provided from Shanghai Fourth Chemical Reagent Company (China). All of the aromatic aldehydes (Benzaldehyde, 4-nitrobenzaldehyde, 4-methoxybenzaldehyde, 1-naphthaldehyde and 3,5-di-tert-butylbenzaldehyde) were purchased from Beijing Innochem Science & Technology Co., Ltd.. Stock solution (2×10^{-2} M) of the aqueous nitrate salts of Li^+, Na^+, K^+, Mg^{2+}, Ca^{2+}, Sr^{2+}, Ba^{2+}, Co^{2+}, Ni^{2+}, Cu^{2+}, Mn^{2+}, Zn^{2+}, Cd^{2+}, Fe^{2+}, Ag^+, Pb^{2+}, Al^{3+}, Cr^{3+}, Fe^{3+} and Hg^{2+} were prepared for further experiments.

Instruments and spectroscopic measurements: The elemental analyses of C, H and N were performed on a Vario EL III elemental analyzer. ^1H NMR spectra were measured on a Bruker-400 spectrometer with Me_4Si as an internal standard. X-Ray powder diffraction (XRD) patterns of the Cd-MDIP was recorded on a Rigaku D/max-2400 X−ray powder diffractometer (Japan) using Cu-*K*α (λ = 1.5405 Å) radiation. FT−IR spectra were recorded as KBr pellets on JASCO FT/IR−430. Thermogravimetric analysis (TGA) was carried out at a ramp rate of 5 °C/min in a nitrogen flow with a Mettler-Toledo TGA/SDTA851 instrument. Fluorescence spectra of the solution were obtained using the F−4600 spectrometer (Hitachi). Both excitation and emission slit widths were 5 nm. Fluorescence measurements were carried out in a 1 cm quartzcuvette with stirring the suspension of Cd-MDIP. The adsorption abilities of Cd-MDIP for Fe^{3+} in water was measured by Inductively Coupled Plasma Spectrometer (Perkin Elmer).

Table S1 Selective bond distance (Å) and angle (°) in Cd-MDIP.

Cd(1)–O(1W)	2.271(7)	Cd(1)–O(2B)	2.323(4)
Cd(1)–O(2)	2.323(4)	Cd(1)–O(1)	2.372(3)
Cd(1)–O(1B)	2.372(3)	Cd(1)–O(2W)	2.452(6)
Cd(1)–O(2WA)	2.454(4)		
O(1W)–Cd(1)–O(2B)	88.64(11)	O(1W)–Cd(1)–O(2)	88.64(11)
O(2B)–Cd(1)–O(2)	158.03(17)	O(1W)–Cd(1)–O(1)	96.06(18)
O(2B)–Cd(1)–O(1)	146.66(11)	O(2)–Cd(1)–O(1)	55.31(11)
O(1W)–Cd(1)–O(1B)	96.07(18)	O(2B)–Cd(1)–O(1B)	55.31(11)
O(2)–Cd(1)–O(1B)	146.66(11)	O(1)–Cd(1)–O(1B)	91.35(16)
O(1W)–Cd(1)–O(2W)	173.9(2)	O(2B)–Cd(1)–O(2W)	90.19(10)
O(2)–Cd(1)–O(2W)	90.19(10)	O(1)–Cd(1)–O(2W)	88.21(13)
O(1B)–Cd(1)–O(2W)	88.20(13)	O(1W)–Cd(1)–O(2WA)	96.0(2)
O(2B)–Cd(1)–O(2WA)	79.30(8)	O(2)–Cd(1)–O(2WA)	79.30(8)
O(1)–Cd(1)–O(2WA)	132.53(8)	O(1B)–Cd(1)–O(2WA)	132.53(8)
O(2W)–Cd(1)–O(2WB)	77.90(18)		

Symmetry code A: *x*, -*y*, 1-*z*; B: -*x*, *y*, *z*.

Figure S1. The fluorescence spectra of Cd-MDIP in water solution upon the addition of 0.55 mM of various metal ions.

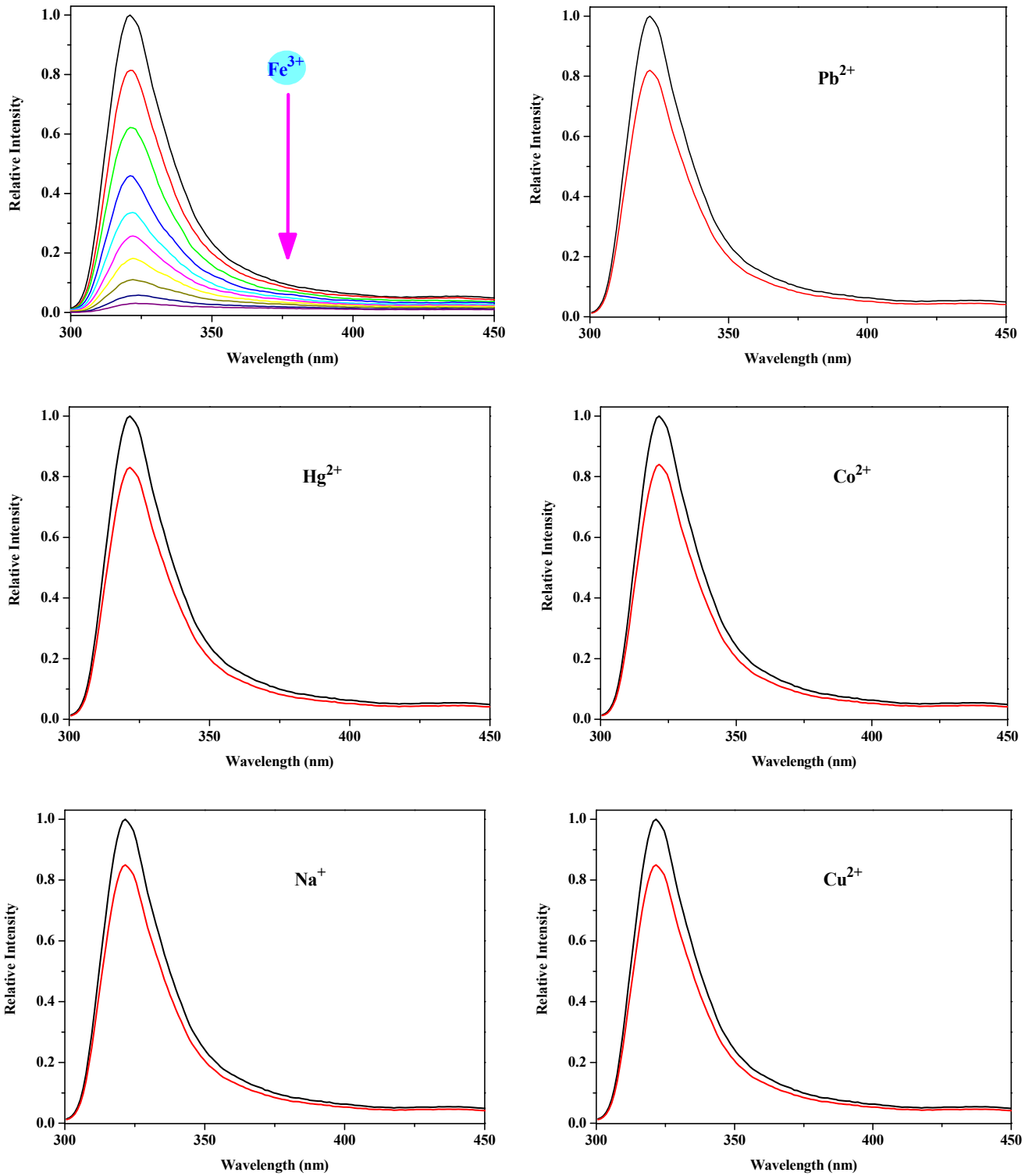

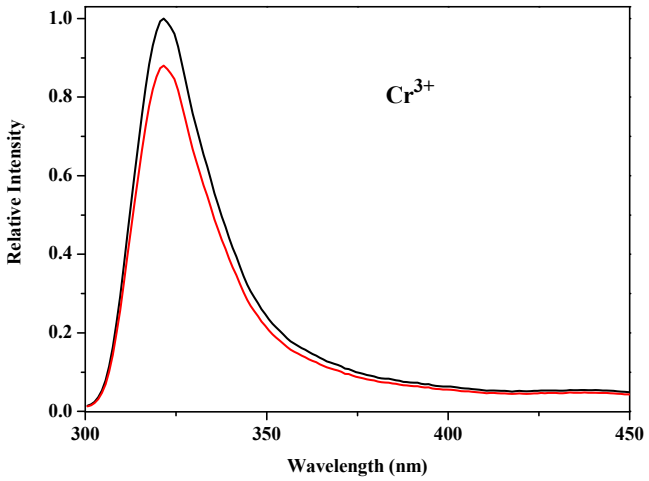
Cr3+
Relative Intensity
Wavelength (nm)
1.0
0.8
0.6
0.4
0.2
0.0
300
350
400
450

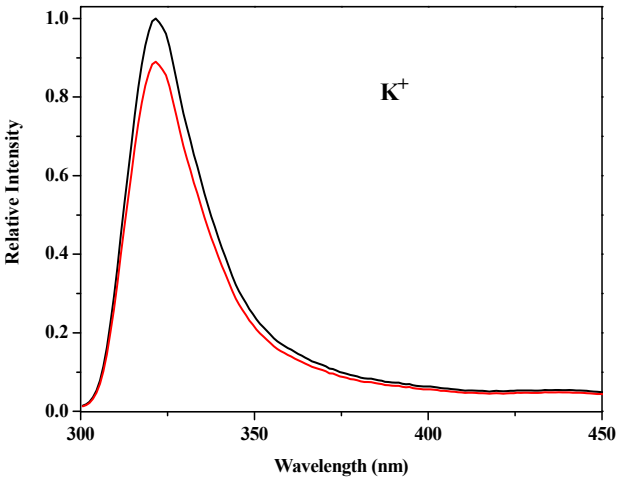
K+
Relative Intensity
Wavelength (nm)
1.0
0.8
0.6
0.4
0.2
0.0
300
350
400
450

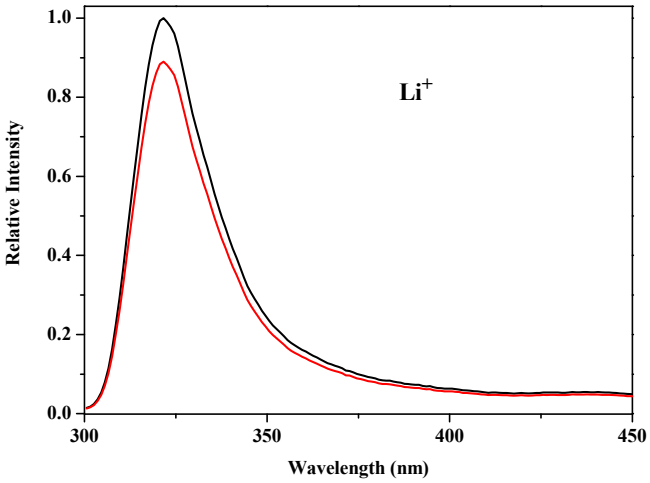
Li+
Relative Intensity
Wavelength (nm)
1.0
0.8
0.6
0.4
0.2
0.0
300
350
400
450

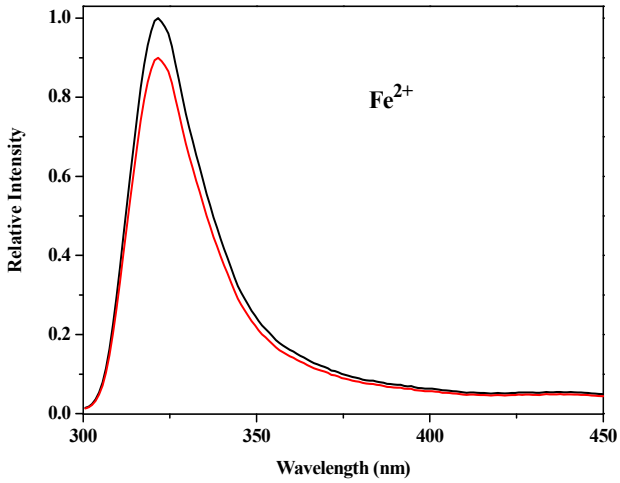
Fe2+
Relative Intensity
Wavelength (nm)
1.0
0.8
0.6
0.4
0.2
0.0
300
350
400
450

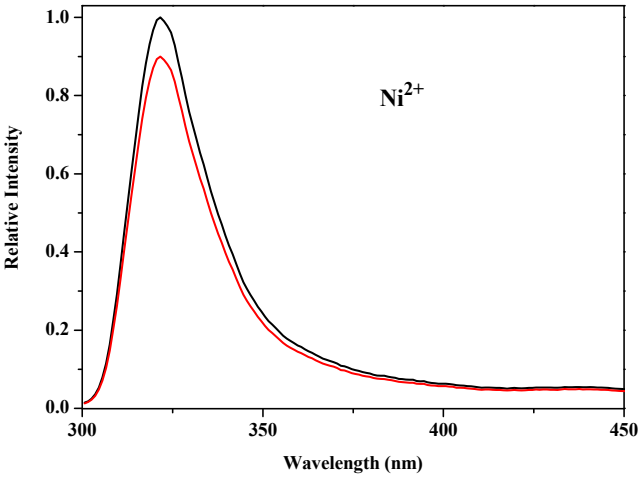
Ni2+
Relative Intensity
Wavelength (nm)
1.0
0.8
0.6
0.4
0.2
0.0
300
350
400
450

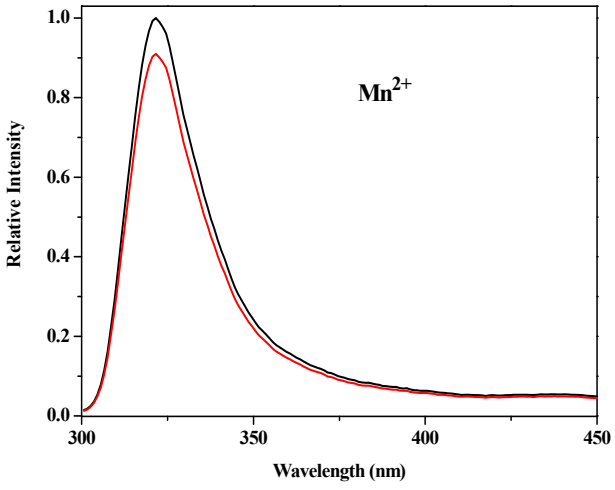
Mn2+
Relative Intensity
Wavelength (nm)
1.0
0.8
0.6
0.4
0.2
0.0
300
350
400
450

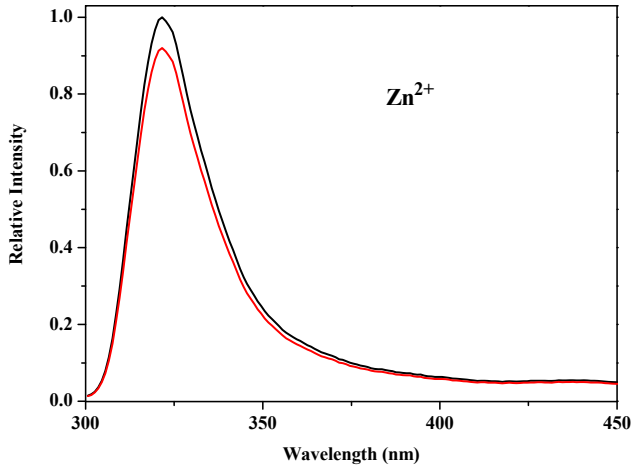
Zn2+
Relative Intensity
Wavelength (nm)

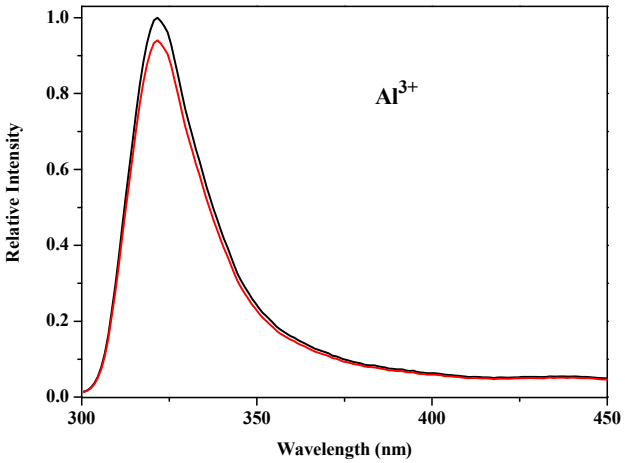
Al3+
Relative Intensity
Wavelength (nm)

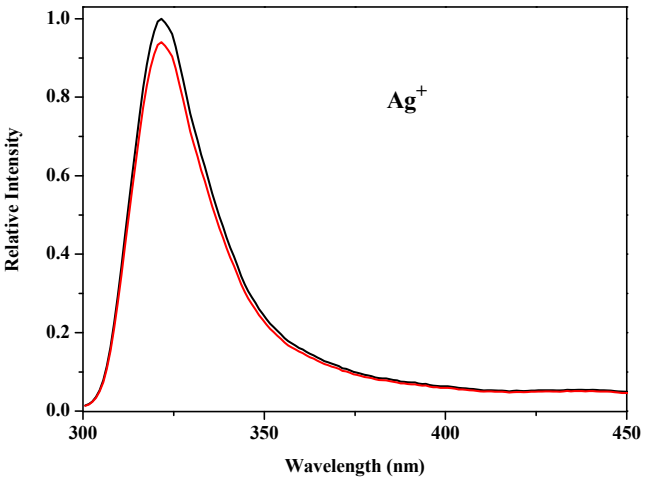
Ag+
Relative Intensity
Wavelength (nm)

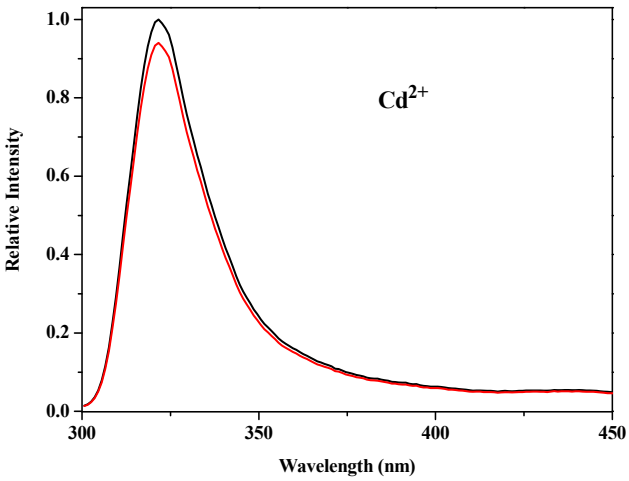
Cd2+
Relative Intensity
Wavelength (nm)

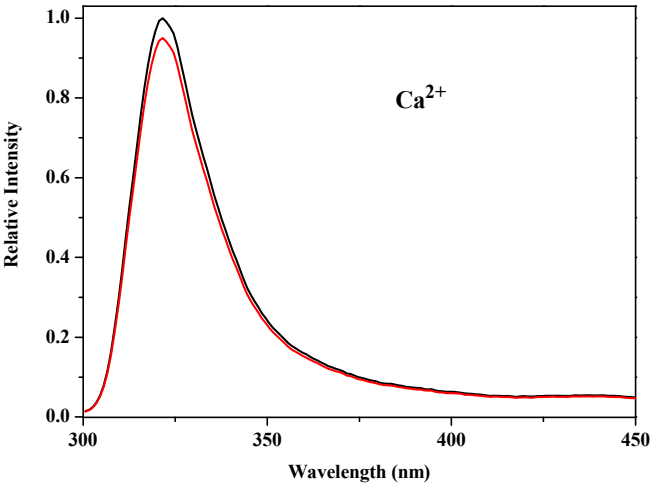
Ca2+
Relative Intensity
Wavelength (nm)

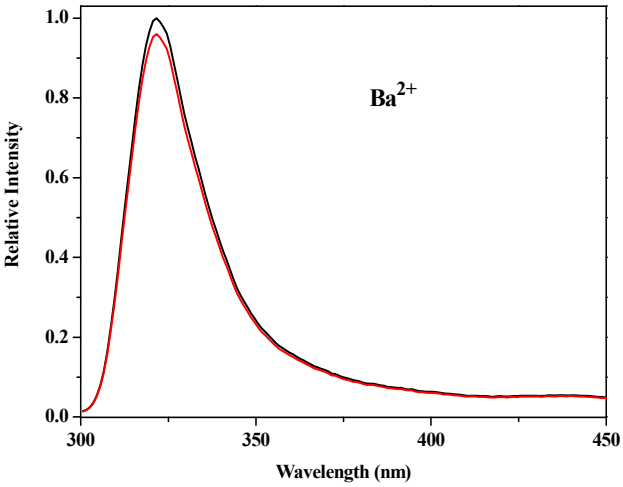
Ba2+
Relative Intensity
Wavelength (nm)

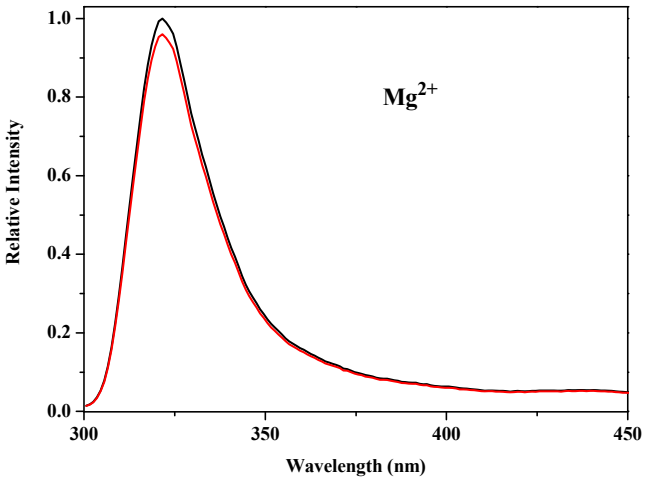
Mg2+
Relative Intensity
Wavelength (nm)
1.0
0.8
0.6
0.4
0.2
0.0
300
350
400
450

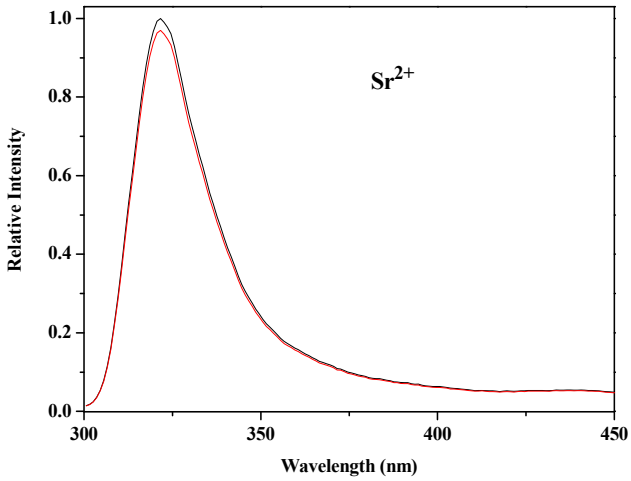
Sr2+
Relative Intensity
Wavelength (nm)
1.0
0.8
0.6
0.4
0.2
0.0
300
350
400
450

Figure S2. The Stern−Volmer plot of Cd-MDIP quenched by Fe^{3+} aqueous solution, where I_0 and I are the fluorescence intensity ratio before and after metal ion incorporation, respectively.

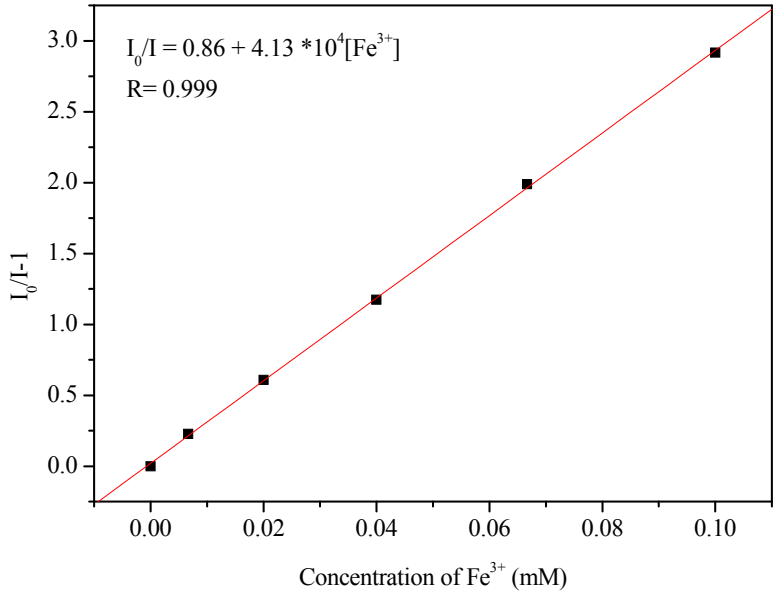

Figure S3. The DR UV−vis spectra of Cd−MDIP, $Fe(NO_3)_3$ and Cd−MDIP⊃Fe^{3+}.

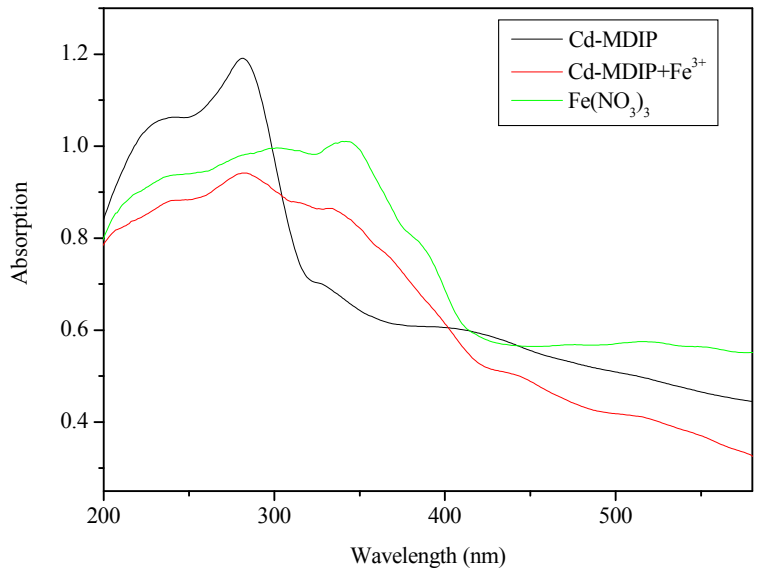

Table S1. The ICP results of splitting Cd−MDIP (2 mg), splitting of Cd−MDIP (2 mg) after treated with excess Fe^{3+} in 50 mL solution, respectively.

	$[Cd^{2+}]$ (μM)	$[Fe^{3+}]$ (μM)
splitting Cd−MDIP	76.7	
splitting Cd−MDIP after treated with Fe^{3+}	76.5	4.5

Figure S4. The PXRD pattern of the residue left of Cd-MDIP and Cd-MDIP⊃Fe^{3+} behind were found to be predominantly CdO phase and CdO + Fe_3O_4 mixture phase, respectively.

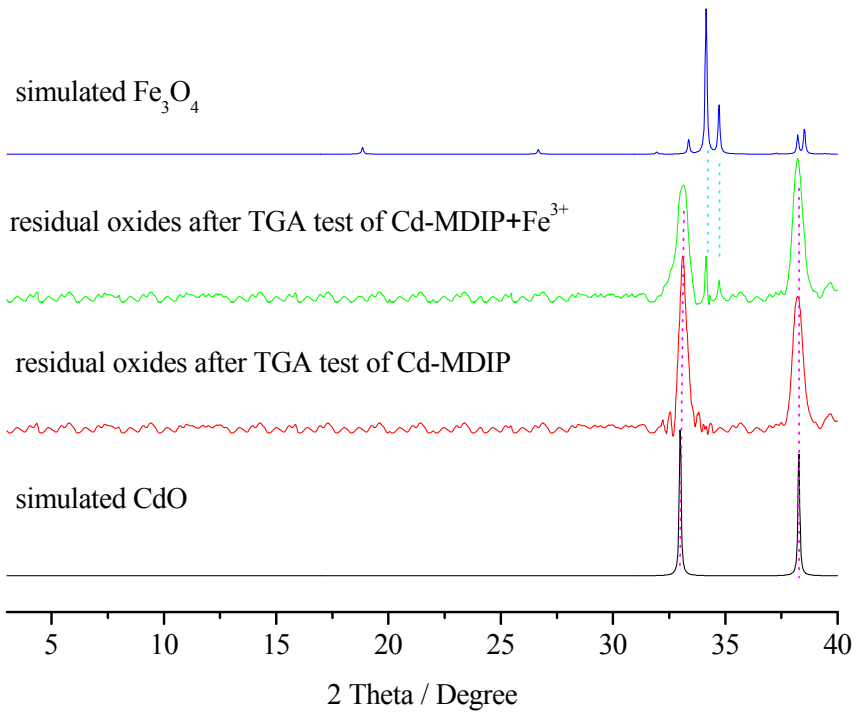

Figure S5. Study on recycling of catalyst Cd-MDIP⊃Fe^{3+} for the heterogeneous cyanosilylation: $(CH_3)_3SiCN$: 1.2 mmol; benzaldehyde: 0.5 mmol; Cd-MDIP⊃Fe^{3+} catalysts: 2.5 μmol, room temperature for 2 hours.

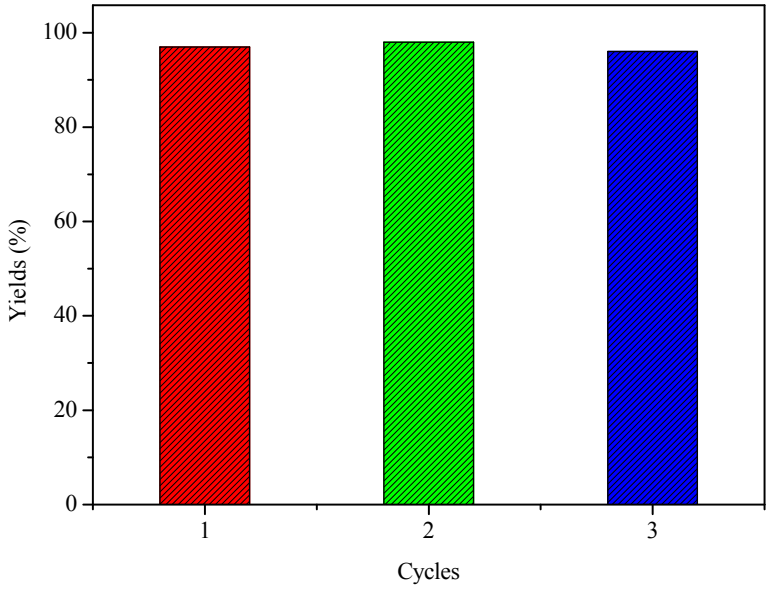

Figure 6. ^1H NMR (400 MHz, $CDCl_3$) of 2-phenyl-2-(trimethylsilyloxy)-acetonitrile.

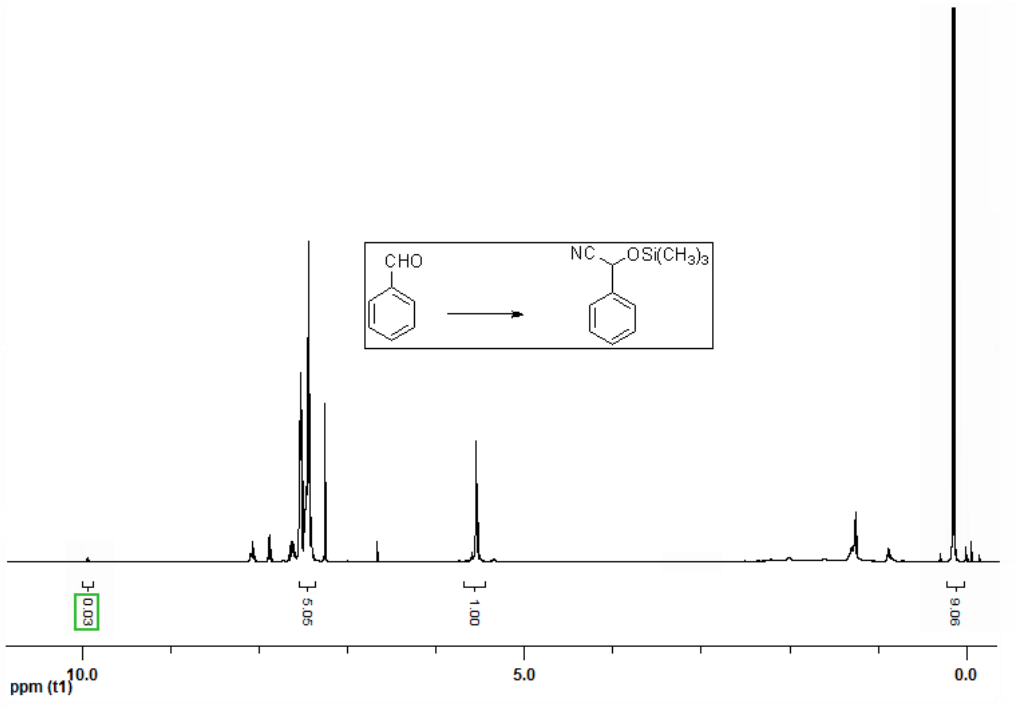

Figure S7. ^{1}H NMR (400 MHz, $CDCl_3$) of 2-(4-nitrophenyl)-2-((trimethylsilyl)oxy)-acetonitrile.

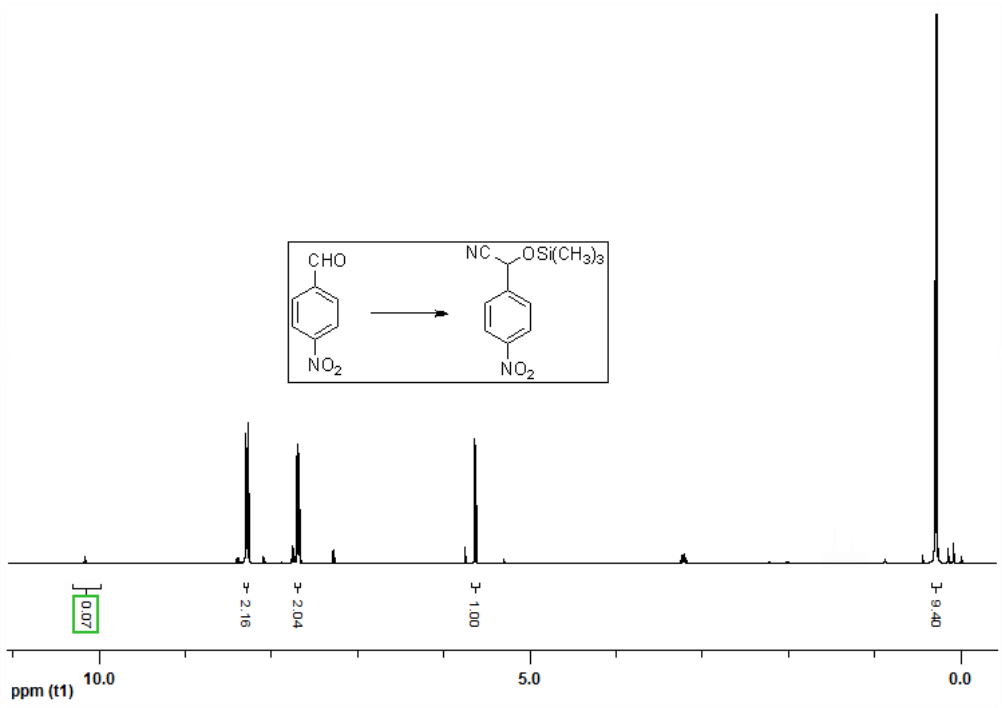

Figure S8. ^{1}H NMR (400 MHz, $CDCl_3$) of 2-(4-methoxyphenyl)-2-(trimethylsilyloxy)-acetonitrile.

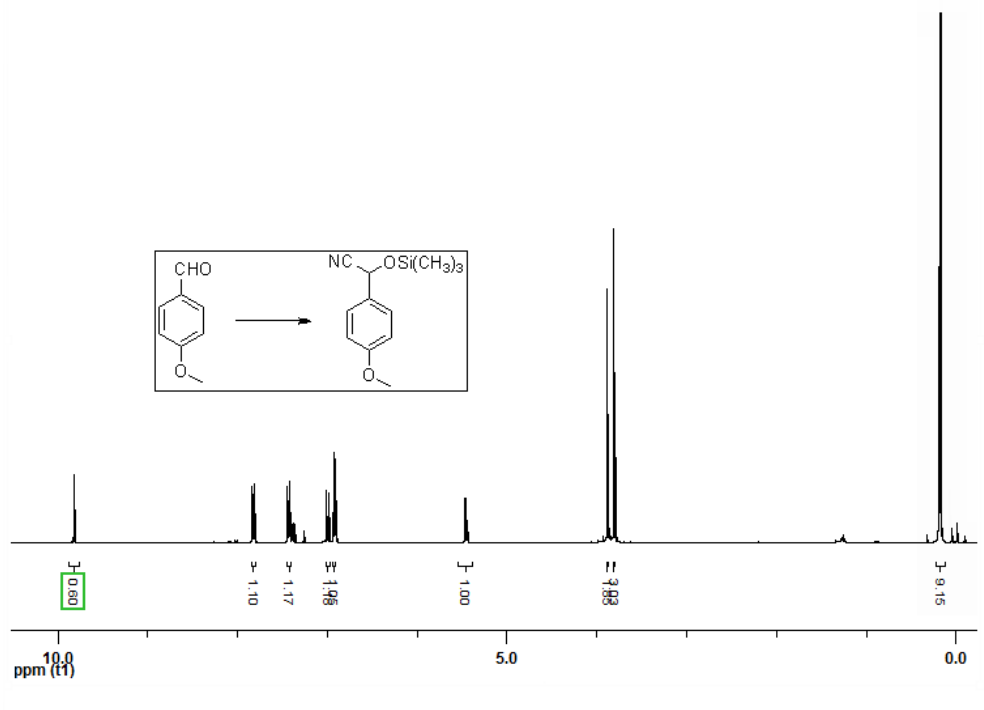

Figure S9. ^{1}H NMR (400 MHz, $CDCl_3$) of 2-(naphthalene-1-yl)-2-(trimethylsilyloxy)-acetonitrile.

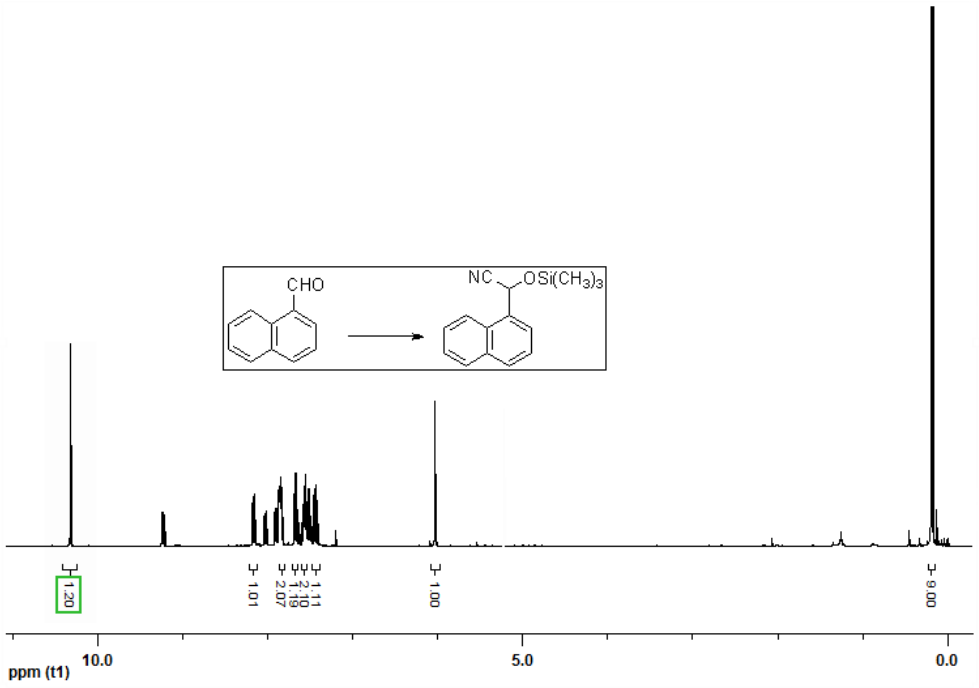

Table S2. Comparison with different MOF catalysts in the catalytic of cyanosilylation reaction of benzaldehyde with $(CH_3)_3SiCN$.

Entry	Catalyst	T (℃)	t (hr)	Yield(%)	Ref.
1	1·Cd	r.t.	18	94	[S1]
2	Cd-PBA	r.t.	8	99	[S2]
3	Ce-MDIP1	r.t.	24	93	[S3]
4	Ce-MDIP2	r.t.	24	94	[S3]
5	Eu-PDC	r.t.	3	93	[S4]
6	MIL-47 (V)	r.t.	3	46	[S5]
7	MIL-53 (Al)	r.t.	3	26	[S5]
8	MIL-101 (Cr)	r.t.	4	96	[S5]
9	Zn-MOF	r.t.	10	74	[S6]
10	Ce-MOF	r.t.	2	94	[S7]
11	Ps-CMOF	r.t.	48	93	[S8]
12	POMOF-1	r.t.	24	98	[S9]
13	UPC-15	r.t.	24	99	[S10]
14	UPC-16	r.t.	24	97	[S10]
15	Co-MOF	r.t.	12	98	[S11]
16	Cd-bpdc	r.t.	14	95	[S12]
17	Mn-MOF	r.t.	9	98	[S13]
18	Cd-MDIP⊃Fe^{3+}	r.t.	2	97	This work

Reference

S1. W. Jiang, J. Yang, Y.-Y. Liu, S.-Y. Song, J.-F. Ma, *Inorg. Chem.*, 2017, **56**, 3036.

S2. L. Hu, G.-X. Hao, H.-D. Luo, C.-X. Ke, G. Shi, J. Lin, X.-M. Lin, U. Y. Qazi, Y.-P. Cai, *Cryst. Growth Des.*, 2018, DOI: 10.1021/acs.cgd.7b01728.

S3. D. Dang, P. Wu, C. He, Z. Xie, C. Duan, *J. Am. Chem. Soc.*, 2010, **132**, 14321.

S4. X.-M. Lin, J.-L. Niu, P.-X. Wen, Y. Pang, L. Hu, Y.-P. Cai, *Cryst. Growth Des.*, 2016, **16**, 4705.

S5. Z. Zhang, J. Chen, Z. Bao, G. Chang, H. Xing, Q. Ren, *RSC Adv.*, 2015, **5**, 79355.

S6. A. Karmakar, A. Paul, G. M. D. M. Rúbio, M. F. C. G. da Silva, A. J. L. Pombeiro, *Eur. J. Inorg. Chem.*, 2016, **2016**, 5557.

S7. A. Karmakar, G. M. D. M. Rubio, A. Paul, M. F. C. G. da Silva, K. T. Mahmudov, F. I. Guseinov, S. A. C. Carabineiro, A. J. L. Pombeiro, *Dalton Trans.*, 2017, **46**, 8649.

S8. J. Li, Y. Ren, C. Qi, H. Jiang, *Chem. Commun.*, 2017, **53**, 8223.

S 9. Q. Han, X. Sun, J. Li, P. Ma, J. Niu, *Inorg. Chem.*, 2014, **53**, 6107.

S10. X. Wang, L. Zhang, J. Yang, F. Dai, R. Wang, D. Sun, *Chem. Asian J.*, 2015, **10**, 1535.

S11. X. Cui, M.-C. Xu, L.-J. Zhang, R.-X. Yao, X.-M. Zhang, *Dalton Trans.*, 2015, **44**, 12711.

S12. A. Bhunia, S. Dey, J. M. Moreno, U. Diaz, P. Concepcion, K. Van Hecke, C. Janiak, P. Van Der Voort, *Chem. Commun.*, 2016, **52**, 1401.

S13. S. Horike, M. Dincă, K. Tamaki, J. R. Long, *J. Am. Chem. Soc.*, 2008, **130**, 5854.